LA-UR- 10-01950

Approved for public release; distribution is unlimited.

Title: The Study of High-Speed Surface Dynamics using a Pulsed Proton Beam

Author(s): W. T. Buttler, D. M. Oro, G. Dimonte, and C. Morris

Intended for: Defense Science Quarterly

Los Alamos
NATIONAL LABORATORY
EST. 1943

Los Alamos National Laboratory, an affirmative action/equal opportunity employer, is operated by the Los Alamos National Security, LLC for the National Nuclear Security Administration of the U.S. Department of Energy under contract DE-AC52-06NA25396. By acceptance of this article, the publisher recognizes that the U.S. Government retains a nonexclusive, royalty-free license to publish or reproduce the published form of this contribution, or to allow others to do so, for U.S. Government purposes. Los Alamos National Laboratory requests that the publisher identify this article as work performed under the auspices of the U.S. Department of Energy. Los Alamos National Laboratory strongly supports academic freedom and a researcher's right to publish; as an institution, however, the Laboratory does not endorse the viewpoint of a publication or guarantee its technical correctness.

Form 836 (7/06)

The Study of High-Speed Surface Dynamics using a Pulsed Proton Beam by W. T. Buttler, D. M. Oro, G. Dimonte, and C. Morris (Los Alamos National Laboratory)

Los Alamos National Laboratory (LANL) is presently engaged in development and implementation of ejecta source term and transport models for integration into LANL hydrodynamic computer codes. Because the underlying postulate for ejecta formation is that ejecta are characterized by a special limiting case of a Richtmyer-Meshkov (RM) instability,[1,2] where the Atwood number is $A = -1$,[3] a key element of the source modeling and transport centers on high-explosive (HE) shocked-Sn validation and verification RM experiments, such as the experimental results presented here.

The FY09 experimental package design, seen in Fig. 1., incorporated a P025 HE lens and a PBX 9501 booster in contact with a Ti buffer onto which the Sn sample was mounted. The HE was confined within a Delrin cylinder that included a Delrin capped Lexan tube that permitted inclusion of seven laser Doppler velocimetry probes positioned to monitor the free-surface velocity in four regions, and the coincident measurement of the RM bubble and spike velocities.

The Ti buffer had an outer diameter, $d = 76.2$ mm and thickness $\tau = 4$ mm, with a 1 mm deep counter-sunk area on the package center-line that was cut to the Sn target diameter of $d = 42$ mm; the Sn target was epoxied into the counter-sunk region. The average Sn target thickness was $\tau = 2$ mm, and had three regions with a sine-wave pattern machined into the surface. The three regions were separated by two flat regions used to determine the shocked surface particle velocity. The three sine-wave areas were defined by two different wavelengths of $\lambda_1 = 0.60$ mm, $\lambda_2 = 2.5$ mm, and $\lambda_3 = 0.60$ mm, with sine-wave amplitudes of $a_1 = 0.025$ mm, $a_2 = 0.10$ mm, and $a_3 = 0.10$ mm. These parameters gave wave-number and amplitude products of $k_1\, a_1 = k_2\, a_2 = 1/4$, and $k_3\, a_3 = 1$.

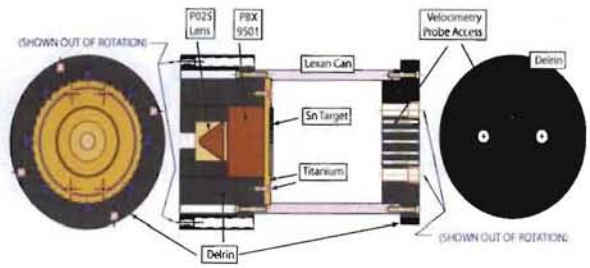

Fig. 1 This figure shows the HE package geometry together with the pressure can assembly.

Earlier work emphasized the need for the Proton Radiograpy (pRad) Facility's ×3 magnification capability, which has a resolution of 100 μm and a 40 by 40 mm square field of view (FOV), to image ejecta formation. Experimental timing was determined through the use of known HE and dtonator function times combined with the expected shockwave pressure P_{SB} and the ejecta velocity model used to estimate the speeds of the fastest ejecta. The ejecta velocity model is based on a Meyer-Blewett approximation,[3] that gives estimates for the ejecta "spike" velocities of

$$u_{spk} = u_{fs} + u_{fs}\frac{ka}{2}\left(2 - \frac{u_{fs}}{u_{sh}}\right) = u_{fs} + u_{mb},$$

where u_{spk} is the fastest spike velocity, u_{mb} is the Meyer-Blewett velocity, u_{fs} is the "free-surface" velocity, ka is the product of the wavenumber and amplitude, and u_{sh} is the velocity of the shockwave within the shocked Sn material. Assuming $P_{SB} \approx 35$ GPa implies $u_{fs} \approx 2.25$ mm/μs and that $u_{sh} \approx 4.27$ mm/μs. Using the largest $ka = 1$ for this system gives $u_{spk} \approx 3.9$ mm/μs. Using the estimated shockwave breakout time together with the FOV and ejecta velocities, three image times were grouped early to capture breakout, and the remaining sixteen were grouped every 700 ns for the experimental duration.

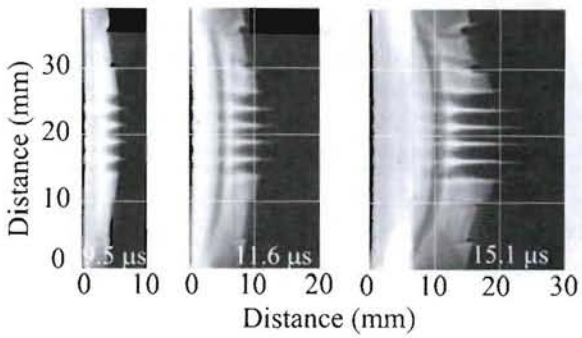

Fig. 2. Three of nineteen FY09 pRad RM images (Shot 371), with image times shown in the lower portion of each image. The instabilities are not fully resolved at this scale and contrast level. However, the salient features that include bubble and spike positions relative to the flat regions are evident.

These preparations led to the vacuum data presented in Fig. 2, which shows the short-wavelength, large-amplitude ($ka = 1$) RM spikes travel the fastest, with the short-wavelength and small-amplitude ($ka = 1/4$) traveling at a similar yet lower velocity as the long-wavelength and large amplitude ($ka = 1/4$). The bubbles are also clearly evident and distinguishable from the free-surface velocity that is determined by the flat regions between the sinusoidal perturbations.

Time-series data are presented in Figs. 3 and 4. Removed from these data are the long-wavelength regions (these data are not useful because the longer

wavelength is on the order of the target thickness τ), and the $\lambda = 600$ μm regions with $a = 25$ μm and $a = 100$ μm are positioned side-by-side. The flat regions that relate u_{fs} were kept, and the time-stamps, which are relative to detonator-breakout, are included in the bottom of each image and are matched as well as possible to the nearest times of other frames. These images are also adjusted for contrast to reveal where the spike-masses are. Because of this, the bubbles are not perfectly resolved, as can be seen in comparisons with Fig. 2, whose contrast is nominally set to the proton transmission.

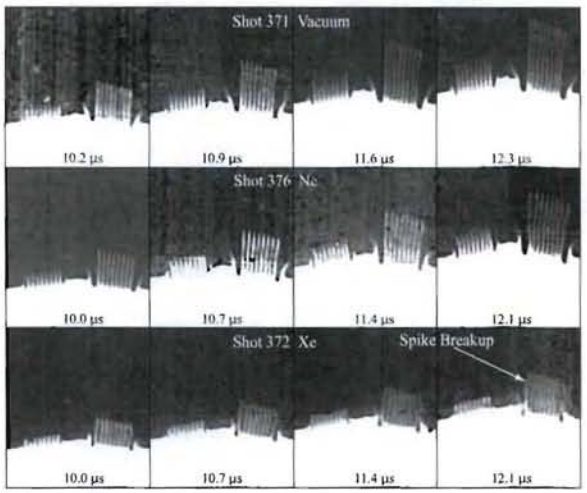

Fig. 3. Vacuum, Ne, and Xe pRad RM time-series data, beginning just after shockwave breakout. The Sn is fully liquid on release, and the gas pressure was ~4 Atm. for each pressurized experiment. Image times are closely matched.

From these data it is seen that the RM spikes in the Ne gas behave much more like the vacuum series than do the spikes in the Xe gas. This is interesting because the viscosity of Ne is about twice the Xe viscosity, i.e., $\eta_{(Ne)} \approx 2\eta_{(Xe)}$. Further, because the density of Xe is about five times the density of Ne, the kinematic viscosity of Ne is about ×10 the kinematic viscosity of Ne: $\eta_{(Ne)}/\rho_{(Ne)} \approx 10\ \eta_{(Xe)}/\rho_{(Xe)}$. The implication is that the Weber number $We = \rho_{Sn} u_{spk}^2 L/\sigma$ dominates the spike-breakup, where L is the spike tip diameter, and σ the surface tension.

The discussion of particle breakup is important to particle transport in gasses. We have highlighted *We*, but we also observe that hydro models predict that the RM spike tips will not continue to grow thinner with time, but rather that they will become blunted due to surface tension. This effect is nominally seen at around 11.6 μs in the vacuum series, which implies the effect happens in the Ne and Xe series as well, but drag may be stripping liquid Sn off the blunted tips, streaming the material toward adjacent neighbors. This assumption is supported by the fact that the RM spikes appear to breakup in the middle of the spikes in the Ne gas at time 15.1 μs, and at time 12.1 μs in the Xe gas. Close inspection reveals that there may be some evidence of the mass streaming from the fastest Ne spike tips, in the shape of a mach-stem, to their nearby neighbors at time 11.4 μs.

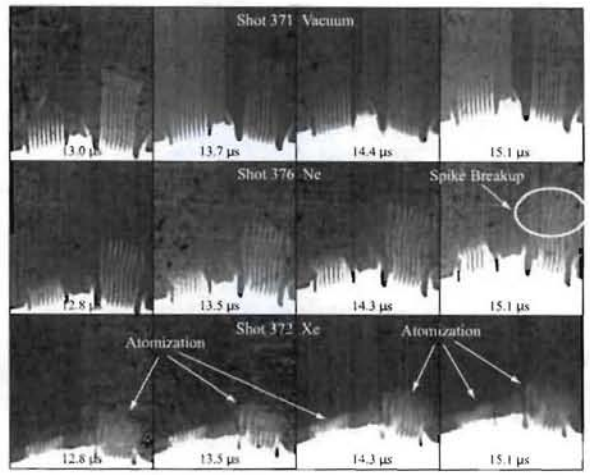

Fig. 4. Additional vacuum, Ne, and Xe pRad RM time-series data. Image times are closely matched.

In conclusion, these observations can be used for code validation and verification studies, and the collection of results to inform FY10 experimental packages. E. g., it is clear that $\lambda = 2.5$ mm is too long for the ×3 magnifier, and too similar in scale to the coupon thickness, for such data to be of value. The results also show that $\lambda = 600$ μm is resolvable, and that it is likely that this can be reduced to $\lambda \approx 450$ μm. The amplitudes are relevant and need not be changed, but the coupon thickness can be increased to as much as $\tau = 10$ mm. It is also possible to reduce the edge release effects by using a larger diameter booster and lens, especially when combined with momentum trapping concepts that isolate release waves from the central portion of the coupon. Other booster materials, such as PBX 9502 or TNT, can be used to reduce the peak stress, P_{SB}, to levels near 20 GPa, allowing full investigation of other components of our ejecta model development.

We acknowledge contributions by Patrick T. Reardon and Machinist Felix P. Garcia of MST-7, and the pRad core team, which is quite extensive.

---

[1]R. D. Richtmyer, Commun. Pure Appl. Math **13**, 297 (1960).

[2]E. E. Meshkov, Izv. Akad. Nauk SSSR, Mekh. Zhidk. Gasa **4**, 151 (1969) [Izf. Acad. Sci. USSR Fluid Dynamics **4**, 101 (1969)].

[3]K. A. Meyer and P. J. Blewett, Phys. Fluids **15**, 753 (1972).